Progress In Electromagnetics Research C, Vol. 114, 185–202, 2021

Digitally Controlled Steered Dual Beam Pattern Synthesis of a Rectangular Planar Array Antenna in a Range of Azimuth Plane Using Evolutionary Algorithms

Sanjay Kr. Dubey[1] and Debasis Mandal[2, *]

Abstract—This paper presents a pattern synthesis method to generate dual-beam patterns of a rectangular planar array of isotropic antennas in a particular scanning angle using Evolutionary Algorithms. The dual-beam patterns are $cosec^2$ pattern and pencil beam pattern, and both the patterns are steered to an elevation angle of 20 degrees ($\theta = 20°$). Moreover, each pattern is synthesized in three azimuth planes ($\varphi = 0°$, $5°$, and $10°$). The isotropic elements are uniformly spaced, and nonuniform excitations are applied to achieve the desired patterns. These patterns are obtained by applying the optimum set of common elements amplitude and phases for the cosecant-squared pattern only. The optimum 4-bit discrete amplitudes and 5-bit discrete phases are produced using Differential Evolutionary (DE) Algorithm, Genetic Algorithm (GA), Particle Swarm Optimization (PSO) Algorithm, and Firefly Algorithm (FA). These discrete excitations are helpful to reduce the Dynamic Range Ratio (DRR) and the design complexity of the feed networks. The excitations are also verified in a range of arbitrarily chosen azimuth planes. The patterns are generated in the same steering angle with minor variations of the desired parameters. The outcomes established the superiority of DE over PSO, GA, and FA and the effectiveness of the proposed method.

1. INTRODUCTION

The array antenna having scanning capability is very useful in wireless communication, mainly in radar-related applications. However, generating the $cosec^2$ beam and pencil beam at a range of azimuth planes along with an elevation angle faced a high sidelobe with an enormous ripple problem. Various approaches reported in literature for generating array patterns and dual beam patterns are as follows [1–11].

Multiple beam patterns using simulated annealing algorithm [5] have been generated by Diaz et al. Lei et al. proposed and developed a process for generating a cosecant-squared beam pattern of a linear antenna array by incorporating optimum amplitudes and phases of the isotropic array elements by applying the modified least square method [6]. Both uniform and Gaussian distributions of common amplitudes are applied to generate shaped beam patterns (flattop and a cosecant-squared). Different sets of phases are also used for different beam patterns. For finding these excitations, the Woodward-Lawson technique [7] has been introduced by Durr et al. Chatterjee et al. proposed a method for generating dual beams using optimum sets of radial amplitudes and phases of a concentric ring array antenna. These excitations are achieved by using Gravitational Search Algorithm (GSA) [8]. Chatterjee et al. also proposed a Firefly Algorithm (FA) technique for generating a dual-beam pattern of a concentric ring antenna array. The applied elements are isotropic, and the excitations are used in the rings of the CCAA instate of the elements. The expected patterns are generated by applying specific states or combinations

Received 23 June 2021, Accepted 29 July 2021, Scheduled 9 August 2021
* Corresponding author: Debasis Mandal (dr.debasis1984@gmail.com).
[1] Department of Electronics and Communication Engineering, Shri Jagdishpradad Jhabarmal Tibrewala University, Jhunjhunu, Rajasthan, India. [2] School of Engineering and Technology, K K University, Nalanda, Bihar, India.

of switches [9]. A dual radiation pattern of the rectangular planar array has been generated at different azimuth planes with zero degrees elevation angle using the evolutionary algorithm by Mandal et al. [10]. A flattop and pencil beam is also generated using common amplitudes distribution and phases for shaped beams at zero degrees elevation by Mandal et al. in 2015 [11]. Kenane et al. proposed a method of synthesizing two different non-uniform antenna arrays Linear and Circular, using Dynamic Invasive Weeds Optimization (IWO), which helps to get deep nulls in the directions of interferences with low sidelobe levels [12].

In this paper, a $cosec^2$ pattern and a pencil beam pattern from a planar array [1–4] of 90 isotropic elements are obtained by finding out the optimum set of common elements amplitudes for both the patterns and a group of phases for $cosec^2$ shaped beam using Evolutionary Algorithms. Here 20° progressive phase has also been applied to scan the beam patterns on that elevation angle. The patterns have been generated in three predefined azimuth planes using the excitations achieved by DE, GA, PSO, and FA. This approach also verifies that the patterns retain their desired parameters within a range of azimuth planes instead of a single φ plane. These are also proved by selecting some arbitrary φ planes and obtained similar patterns by applying the same excitations for each Evolutionary Algorithm with some minor variations. The received amplitudes (4-bit) and phases (5-bit) are both digitals for providing a lower Dynamic Range Ratio (DRR). These discrete excitations are used to shorten the design complexity of the feed network as DRR is less, so less number of attenuators and phase shifters are required. The comparative performance of these four Evolutionary Algorithms, Differential Evolution algorithms (DE), Genetic Algorithm, Particle Swarm optimization algorithms, and Firefly Algorithm (FA) are also analyzed.

2. PROBLEM FORMULATIONS

A planar array of 90 isotropic elements is considered. The far-field pattern of the array shown in Figure 1 can be written as [1–4]:

$$AF(\theta,\varphi)=\sum_{m=1}^{M}\sum_{n=1}^{N}I_{mn}e^{j[kmd_x(\sin\theta\cos\varphi-\sin\theta_o\cos\varphi_o)+knd_y(\sin\theta\sin\varphi-\sin\theta_o\sin\varphi_o)+\alpha_{mn}]} \tag{1}$$

Here,
I_{mn} is the excitation amplitude of mn-th element;
α_{mn} denotes the phase excitation of mn-th element;
M and N denote the number of isotropic elements in X and Y directions, respectively;
d_x and $d_y = 0.5\lambda$ represent the inter element spacing along with X and Y directions;

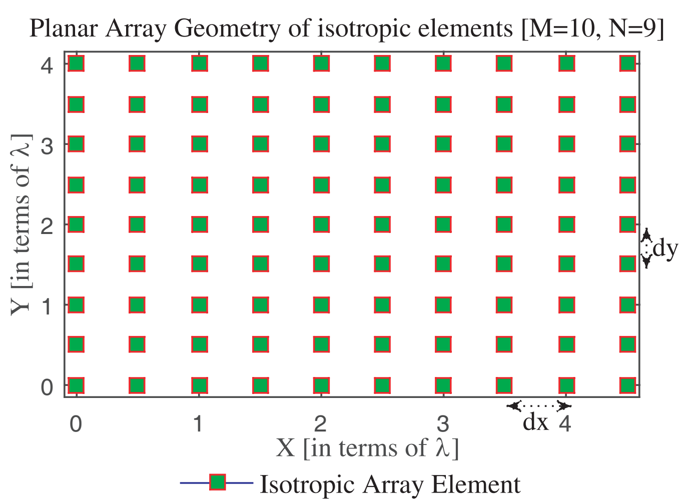

Figure 1. Geometry of a planar array of 90 isotropic elements.

θ and φ are polar and azimuth angle;
θ_o and φ_o are beam pointing angle;
$k = \frac{2\pi}{\lambda}$ is the wavenumber.

The fitness function for the dual-beam pattern ($cosec^2$ and Pencil Beam) is defined as:

$$F(\rho) = k_1 \left\{ peakSLL^{d_1} - \max_{\theta \in S_1} \left\{ AF^{\rho}_{dB}(\theta, \varphi) \right\} \right\}^2 + k_2 \times \triangle + k_3 \left\{ peakSLL^{d_2} - \max_{\theta \in S_2} \left(AF^{\rho}_{dB}(\theta, \varphi) \right) \right\}^2 \quad (2)$$

where Δ is defined as:

$$\Delta = \sum_{\theta_{ripple} \in \{0^\circ + \theta_0 - 30^\circ + \theta_0\}} \left| AF^{\rho}_{dB}(\theta_{ripple}, \varphi) - D(\theta_{ripple}, \varphi) \right| \quad (3)$$

In Equations (2) and (3) $\varphi \in (0^\circ\text{–}10^\circ)$ plane.

ρ is the unknown parameter set responsible for the desired beam patterns for this approach. ρ is defined as follows:

$$\rho = \{I_{mn}, \alpha_{mn}\}; \qquad 1 \le m \le M \ \& \ 1 \le n \le N \quad (4)$$

$peakSLL^{d_1}$ and $peakSLL^{d_2}$ are the desired values of peak SLL for $cosec^2$ and pencil beam patterns. S_1 and S_2 are sidelobe regions for both patterns. $D_{dB}(\theta, \phi)$ is the desired pattern shown in Figure 2 at ($\theta_o = 20^\circ$, $\varphi = 0^\circ$), ($\theta_o = 20^\circ$, $\varphi = 5^\circ$), and ($\theta_o = 20^\circ$, $\varphi = 10^\circ$) planes. The range of θ_{ripple} for this approach is 20° to 50°. k_1, k_2, and k_3 are the weighting factors. This fitness function has to be minimized by finding out the optimum set of 4-bit amplitudes and 5-bit phases using Different Evolutionary Algorithms like Differential Evolution algorithm (DE), Genetic Algorithm (GA), Particle Swarm Optimization Algorithm (PSO), and Firefly Algorithm (FA).

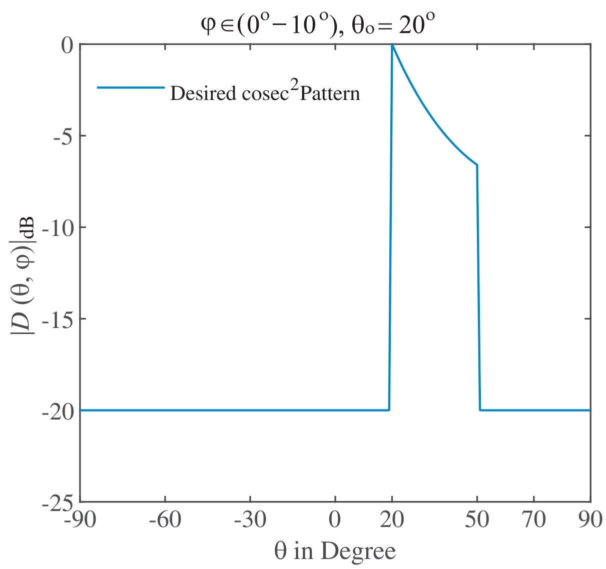

Figure 2. Desired $cosec^2$ pattern for predefined planes $\varphi \in (0^\circ\text{–}10^\circ)$ and $\theta_o = 20^\circ$.

3. EVOLUTION ALGORITHM (EA)

3.1. An Overview of Differential Evolution Algorithm (DE)

Based on the natural evolution of several species, an Evolutionary Algorithm (EA) is proposed and used to solve various optimization problems in a large field of applications, where the appropriate encoding schemes, evolutionary operators, and suitable parameter setting are necessary. In 1997, Differential Evolution (DE) Algorithm, the best population-based Evolutionary Algorithm (EA), was introduced by Storn and Price. The most common Evolutionary Algorithms (EA) are Genetic Algorithms (GA),

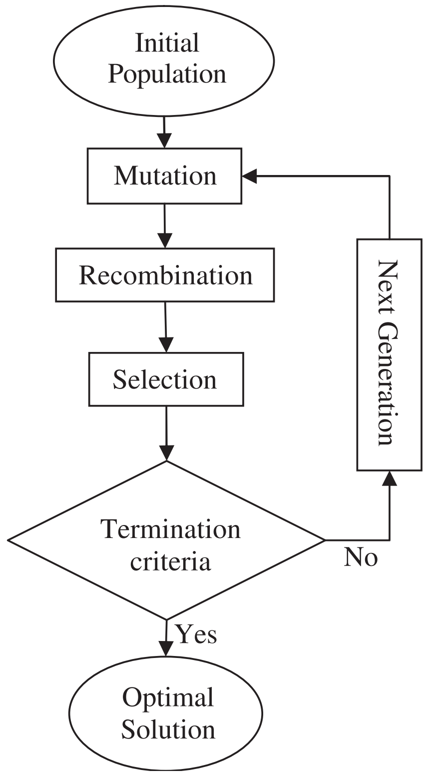

Figure 3. Flow chart of Differential Evolution Algorithm (DE).

Particle Swarm Optimization (PSO), and DE. This Optimization Algorithm DE [13–19] can find out true global minima with fewer control parameters and achieve convergence quickly for nonlinear problems. DE is an efficient and effective global optimizer that is population-based. DE algorithm has used a very powerful stochastic search technique. In DE, three major parameters like population size, scaling factor, and crossover rate are crucially responsible for algorithm's performance. The flowchart of DE is shown in Figure 3. To minimize a function $f(X)$, where,

$$X = [x_1, x_2, x_3, x_4, \ldots, x_D] \tag{5}$$

where D is the search space dimension or number variables. If the population size is considered as N, the population matrix can be expressed as

$$x^g_{n,i} = \left[x^g_{n,1}, x^g_{n,2}, x^g_{n,3}, x^g_{n,4}, \ldots, x^g_{n,D}\right] \tag{6}$$

Here g is the generation and $n = 1, 2, 3, \ldots, N$. Initial population is generated randomly between upper bound (x^U_i) and lower bound (x^U_i). After random initialization and generation in D dimensional search space, the three main steps involved in the DE Algorithm are Mutation, Recombination, and Selection.

In the Mutation process, three different vectors x^g_{r1n}, x^g_{r2n}, and x^g_{r3n} are selected from each parameter vector. Donor vector v^{g+1}_n can be written as follows.

$$v^{g+1}_n = x^g_{r1n} + F\,(x^g_{r2n} - x^g_{r3n}) \tag{7}$$

F is called Scale Factor, and the value is between 0 and 1.

During the Recombination operation the trial vector $u^{g+1}_{n,i}$ is generated using target vector $x^g_{n,i}$ and donor vector $v^{g+1}_{n,i}$. Finally, in the Selection process, the objective function values are compared with each target vector $x^g_{n,i}$ and trial vector $u^{g+1}_{n,i}$. Those who produce the lowest function value, i.e., the best fitness function, are selected for the next generation. These steps are repeated until it reaches the predefined value of generation. The result, i.e., the best solution of the objective function in the current population, is expressed as $X_{best,G}$.

For solving this optimization problem, the population size is considered as 50, the scale factor (F) taken as 0.8, and the crossover rate (CR) of DE chosen as 0.2, whereas the scheme used in this nonlinear problem is $DE/best/1/bin$ with maximum iteration number of 2000 [13–19].

3.2. An Overview of Particle Swarm Optimization Algorithm (PSO)

With the inspiration of social behavior of birds flock, fish school, etc., a population-based stochastic optimization technique is developed by Kennedy and Eberhart in 1995. The name of this optimization algorithm is Particle Swarm Optimization. It utilizes a population of potential solutions to probe the search space concurrently. The individuals are called the particles, and the population is called the swarm in PSO. In the search space, each particle is associated with a position and velocity. As the swarm is a set of N particles, it can be expressed as: $s = \{x_1, x_2, \ldots, x_n\}$, and the position and velocity of a particle in n-dimensional problem is defined as [20–25]

$$x_i = (x_{i1}, x_{i2}, \ldots, x_{in})^T \in A. \quad \text{where, } i = 1, 2, 3, \ldots, N \text{ and } A \text{ is the search space} \tag{8}$$

$$v_i = (v_{i1}, v_{i2}, \ldots, v_{in})^T \quad \text{where, } i = 1, 2, 3, \ldots, N \tag{9}$$

The velocity and positions of the particles are swaps according to the iterations, and these swaps are controlled by the execution of the particles itself and that of the other particles. The algorithm can be summarized as follows:

Step 1: Initialization

The position and velocity of N number of particles are initialized randomly at iteration t using the following equations:

$$x_{ij}(t) = x_{\min} + rand\,(x_{\max} - x_{\min}) \quad \text{for } i = 1, 2, 3, \ldots, N \text{ and } j = 1, 2, 3, \ldots, n \tag{10}$$

$$v_{ij}(t) = \left(-\frac{x_{\max} - x_{\min}}{2} + rand\,(x_{\max} - x_{\min})\right) \quad \text{for } i = 1, 2, 3, \ldots, N \text{ and } j = 1, 2, 3, \ldots, n \tag{11}$$

where $x_{\min}$ and $x_{\max}$ are the lower and upper bounds of the problem. Within the range $[0, 1]$ rand is an uniform random variable.

Step 2: Fitness evolution at the current iteration

Compute the fitness at the current generation for each particle in the swarm, i.e., evaluate $f(x_i)$ for $i = 1, 2, \ldots, N$.

Step 3: Compute $pbest_i$ and $gbest$

At current iteration, $pbest_i$ is the best previous position of the i-th particle, and $gbest$ is the global best position among all the particles present in the swarm using the following equations [20–27]

$$pbest_i(t) = \underset{t}{\arg\min}\, f_i(t) \tag{12}$$

$$gbest(t) = \underset{i}{\arg\min}\, f(pbest_i(t)) \tag{13}$$

Step 4: Update particles position and velocity

Update the velocity and position at iteration t of the particles using the following equations

$$v_{ij}(t+1) = wv_{ij}(t) + c_1 rand_1\,(pbest_{ij}(t) - x_{ij}(t)) + c_2 rand_2\,(gbest_j(t) - x_{ij}(t)) \tag{14}$$

$$x_{ij}(t+1) = x_{ij}(t) + v_{ij}(t+1) \tag{15}$$

for $i = 1, 2, \ldots, N$ and $j = 1, 2, \ldots, n$. Two uniformly distributed random variables $rand_1$ and $rand_2$ have a range in between $[0, 1]$. c_1 and c_2 weighting factors are called cognitive and social parameter. w is known as the inertia weight. It is expressed as:

$$w = w_{\max} - \left(\frac{w_{\max} - w_{\min}}{T}\right) t \tag{16}$$

where $w_{\min}$ and $w_{\max}$ are set to 0.4 and 0.9, and T is the maximum iteration, which restrict the velocity of the particles such that $|v_{ij}(t+1)| \leq v_{\max}$, for $i = 1, 2, \ldots, N$ and $j = 1, 2, \ldots, n$. This is termed as velocity clamping and is accomplished using the equation given bellow:

$$v_{ij}(t+1) = \left\{ \begin{array}{rcl} v_{\max} & if & v_{ij}(t+1) > v_{\max} \\ -v_{\max} & if & v_{ij}(t+1) < -v_{\max} \end{array} \right\} \tag{17}$$

Step 5

Repeat steps 2–5 until iterations reach their maximum limit. Retain the values of *gbest* as the final result. The swarm size of PSO is taken as 50 with the randomly chosen initial population. The values of C_1 and C_2 are considered as 2 [20–27]. The time-varying inertia weight (w) is chosen in the way where the merits are decreased linearly from 0.9 to 0.4. For every particle on the dth dimension the maximum admissible velocity is considered as $0.9r_d$, where r_d is the deflection between the maximum and minimum possible utility of the decision variables on this dth dimension. At a maximum iteration of 2000, the termination condition is considered.

3.3. Parametric Setup of Genetic Algorithm (GA) and Firefly Algorithm (FA)

In GA, the Population size is considered 50, and the two-point crossover schemes are selected. The probabilities of Crossover and mutation are chosen as 0.08 and 0.01. In the Selection process, the

Table 1. Desired and obtained values of design parameters.

Evolutionary Algorithm	**φ in degree**	**Design Parameters**	**$cosec^2$ Pattern Desired**	**$cosec^2$ Pattern Obtained**	**Pencil beam Pattern Desired**	**Pencil beam Pattern Obtained**
DE	$\varphi = 0°$	Peak SLL (dB)	−20.00	−19.4309	−20.00	−19.1101
		△ (dB)	0.00	17.4573	–	–
	$\varphi = 5°$	Peak SLL (dB)	−20.00	−19.2812	−20.00	−19.5790
		△ (dB)	0.00	17.0585	–	–
	$\varphi = 10°$	Peak SLL (dB)	−20.00	−19.3472	−20.00	−19.2337
		△ (dB)	0.00	16.3329	–	–
GA	$\varphi = 0°$	Peak SLL (dB)	−20.00	−19.5038	−20.00	−19.7556
		△ (dB)	0.00	15.5072	–	–
	$\varphi = 5°$	Peak SLL (dB)	−20.00	−20.1736	−20.00	−20.5462
		△ (dB)	0.00	19.2830	–	–
	$\varphi = 10°$	Peak SLL (dB)	−20.00	−20.5360	−20.00	−19.3472
		△ (dB)	0.00	23.6347	–	–
PSO	$\varphi = 0°$	Peak SLL (dB)	−20.00	−16.4613	−20.00	−16.3823
		△ (dB)	0.00	19.1394	–	–
	$\varphi = 5°$	Peak SLL (dB)	−20.00	−16.8319	−20.00	−16.3430
		△ (dB)	0.00	25.4990	–	–
	$\varphi = 10°$	Peak SLL (dB)	−20.00	−18.4748	−20.00	−18.2034
		△ (dB)	0.00	34.7733	–	–
FA	$\varphi = 0°$	Peak SLL (dB)	−20.00	−15.1632	−20.00	−14.6180
		△ (dB)	0.00	23.3948	–	–
	$\varphi = 5°$	Peak SLL (dB)	−20.00	−14.6955	−20.00	−17.7100
		△ (dB)	0.00	28.1375	–	–
	$\varphi = 10°$	Peak SLL (dB)	−20.00	−15.9527	−20.00	−16.6202
		△ (dB)	0.00	16.3810	–	–

Roulette Wheel scheme is thought about for this proposed problem, and the termination condition is chosen as a maximum iteration of 2000. Other parametric setups of the Genetic Algorithm are selected from the recommendation given in [28–32]. In FA number of fireflies 50 is taken, $\beta_0 = 0.20$, $\gamma = 0.25$, $\alpha = 1$, and Search space dimension and Choice of initial population are considered as 48 and random, at a maximum iteration of 2000 [9].

4. RESULTS

A planar array of 90 uniformly placed isotropic elements has been considered. M number of elements are uniformly placed along X direction, and N number of elements are placed along Y direction. where $M = 10$ and $N = 5$ have been chosen. The inter element spacing is considered as 0.5λ, i.e., $d_x = 0.5\lambda$ and $d_y = 0.5\lambda$ shown in Figure 1.

The design parameters of the steered dual-beam patterns along with their corresponding obtained results are shown in Table 1. From Table 1, it has been seen that by applying DE the obtained values of the peak side lobe level for the *cosec*^{2} beam pattern in three different predefined planes are -19.4309 dB, -19.2812 dB, and -19.3472 dB corresponding to their desired value of -20.00 dB. The parameter ripple (Δ) is incorporated to measure the total deviation between the obtained (shown in Figure 4) and desired patterns (shown in Figure 2) within the angular region ($\theta = 20°$–$50°$). The values of ripple (Δ) are 17.4573 dB, 17.0585 dB, and 16.3329 dB for $\varphi = 0°$, $\varphi = 5°$, and $\varphi = 10°$, respectively, whereas for steered pencil beam pattern the obtained values of peak SLL are -19.1101 dB, -19.5790 dB, and -19.2337 dB respectively for the same azimuth planes.

Similarly, Table 1 shows the obtained and desired values of peak SLL and ripple Δ using Genetic

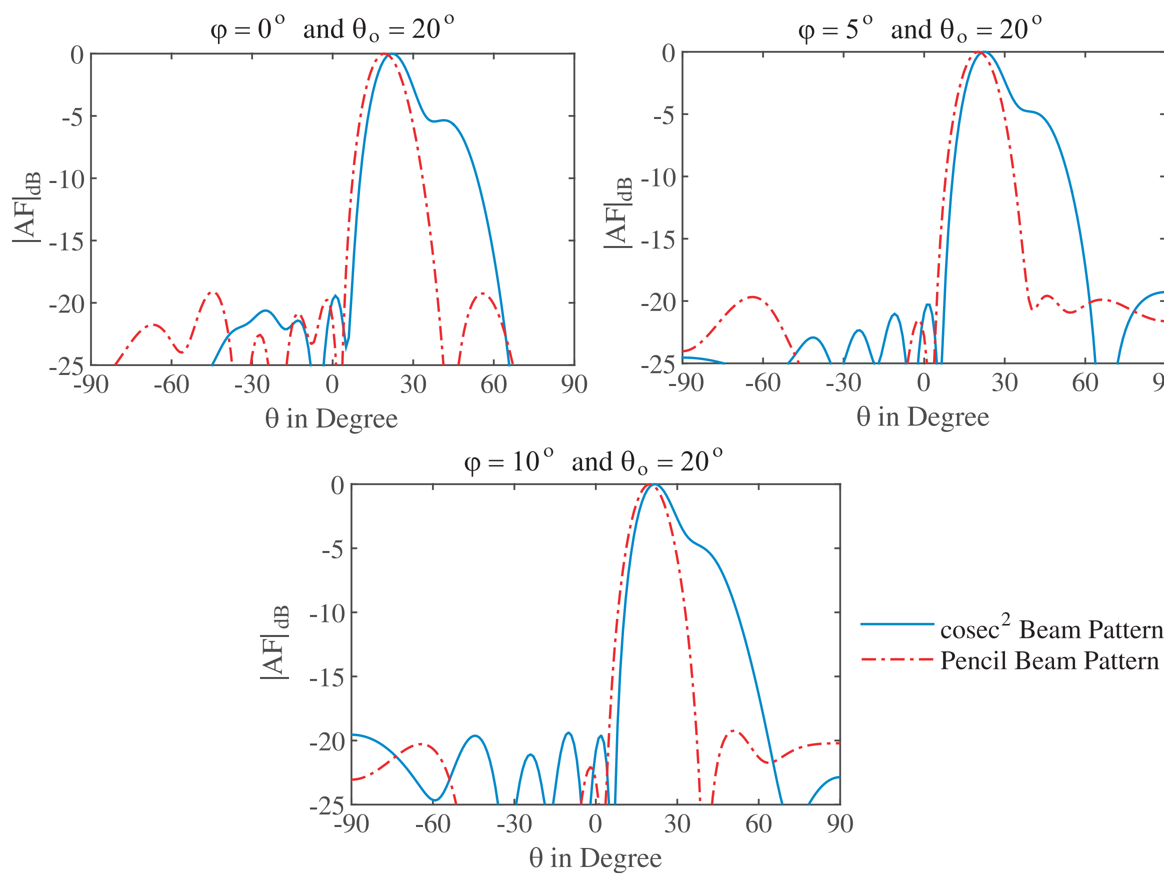

Figure 4. Obtained dual beam patterns at 20° elevation angle using DE for $\varphi = 0°$, $\varphi = 5°$, and $\varphi = 10°$ plane.

Table 2. Obtained results for arbitrary φ planes.

Evolutionary Algorithm	φ in Degree	Design Parameters	$cosec^2$ Pattern	Pencil beam Pattern
DE	$\varphi = 2.7°$	Peak SLL (dB)	−20.0710	−20.3024
		$\triangle$ (dB)	17.0777	–
	$\varphi = 7.8°$	Peak SLL (dB)	−20.0614	−19.4633
		$\triangle$ (dB)	16.0619	–
	$\varphi = 12.1°$	Peak SLL (dB)	−17.8563	−16.6528
		$\triangle$ (dB)	20.7389	–
GA	$\varphi = 2.7°$	Peak SLL (dB)	−20.5479	−21.0475
		$\triangle$ (dB)	18.9636	–
	$\varphi = 7.8°$	Peak SLL (dB)	−20.2494	−19.8361
		$\triangle$ (dB)	19.7764	–
	$\varphi = 12.1°$	Peak SLL (dB)	−20.6196	−16.1608
		$\triangle$ (dB)	34.1074	–
PSO	$\varphi = 2.7°$	Peak SLL (dB)	−16.2464	−15.2728
		$\triangle$ (dB)	22.8719	–
	$\varphi = 7.8°$	Peak SLL (dB)	−17.5902	−17.5627
		$\triangle$ (dB)	27.9257	–
	$\varphi = 12.1°$	Peak SLL (dB)	−14.9866	−11.7208
		$\triangle$ (dB)	46.5058	–
FA	$\varphi = 2.7°$	Peak SLL (dB)	−14.6836	−16.4585
		$\triangle$ (dB)	49.5750	–
	$\varphi = 7.8°$	Peak SLL (dB)	−15.5592	−17.8772
		$\triangle$ (dB)	43.4963	–
	$\varphi = 12.1°$	Peak SLL (dB)	−15.8034	−14.1420
		$\triangle$ (dB)	44.7144	–

Algorithm, Particle Swarm Optimization algorithm, and Firefly Algorithm. Using GA the obtained peak SLLs for the $cosec^2$ patterns in three azimuth planes 0°, 5°, and 10° are −19.5038 dB, −20.1736 dB, and −20.5360 dB corresponding to their ripple values 15.5072 dB, 19.2830 dB, and 23.6347 dB, respectively. The obtained values for both DE and GA meet the expected values of design specifications with some ripple. For the case of PSO and FA, the obtained values of both peak SLL and ripple for both patterns have larger deviation than DE and GA. Figure 4, Figure 5, Figure 6, and Figure 7 depict the obtained steered dual-beam patterns using DE, GA, PSO, and FA, respectively.

The element wise amplitudes and phases of the array elements obtained using DE for generating the beam patterns are shown in Figure 8, and their corresponding values of normalized amplitudes and phases are written in Table 3. These normalized amplitudes have 2^4, i.e., 16 different levels between 0.625 and 1. Similarly, the phases have 2^5, i.e., 32 different levels between −180° and +180°. Figure 9 and Figure 10 show the 4-bit discrete amplitudes and 5-bit discrete phases using GA and PSO. The exact value of discrete 4-bit amplitudes and 5-bit phases are given in Table 4 and Table 5.

Table 3. Element wise excitations using Differential Evolution Algorithm (DE).

Excitations	X→1	2	3	4	5	6	7	8	9	10	Y↓
Amplitude	0.5000	1.0000	0.7500	0.0625	0.0625	0.0625	0.1875	0.3125	0.1875	0.6250	1
Phase	56.25	−45.00	112.50	−157.50	−11.25	180.00	−22.50	157.50	0	112.50	
Amplitude	0.7500	1.0000	0.8125	1.0000	1.0000	0.7500	0.8750	0.8750	0.4375	1.0000	2
Phase	90.00	168.75	157.50	157.50	123.75	67.50	180.00	168.75	180.00	−180.00	
Amplitude	0.4375	1.0000	0.8125	0.4375	0.9375	0.4375	0.3750	0.3125	0.5000	1.0000	3
Phase	−180.00	−168.75	180.00	−180.00	−90.00	−180.00	−157.50	180.00	−123.75	−146.25	
Amplitude	0.1875	0.0625	0.3125	0.0625	0.2500	0.0625	0.1875	0.7500	0.1250	0.0625	4
Phase	-168.75	−180.0	90.00	180.00	146.25	135.00	180.00	180.00	−180.00	168.75	
Amplitude	0.0625	0.0625	1.0000	0.9375	0.8125	0.1250	0.0625	0.1875	0.8750	0.3750	5
Phase	180.00	−78.75	−67.50	11.250	−78.75	−22.50	−101.25	180.00	180.00	−112.50	
Amplitude	0.5625	0.3125	0.0625	0.3750	0.1250	1.0000	1.0000	1.0000	0.3125	0.0625	6
Phase	−78.75	157.50	−112.50	−112.50	−146.25	−180.00	−11.25	180.00	−180.00	180.00	
Amplitude	0.8750	0.7500	0.5625	1.0000	0.6250	0.7500	0.8750	0.9375	1.0000	0.7500	7
Phase	−180.00	−90.00	157.50	180.00	−180.00	112.50	−180.00	180.00	123.75	123.75	
Amplitude	0.0625	0.4375	0.0625	1.0000	1.0000	1.0000	0.8750	0.6250	0.7500	0.4375	8
Phase	−157.50	11.25	−135.00	−180.00	−180.00	180.00	180.00	78.75	−180.00	−123.75	
Amplitude	0.1875	0.8750	0.7500	1.0000	0.9375	0.7500	0.4375	0.4375	0.4375	0.3750	9
Phase	180.00	67.500	146.25	−180.00	−157.50	−123.75	−135.00	180.00	168.75	180.00	

Table 4. Element wise excitations using Genetic Algorithm (GA).

Excitations	X→1	2	3	4	5	5	7	8	9	10	Y↓
Amplitude	0.4375	0.6250	0.9375	0.8750	0.8125	0.8750	0.7500	0.4375	0.3750	0.3125	1
Phase	180.00	78.750	157.50	−168.75	112.50	−78.75	−45.00	−123.75	146.25	90.000	
Amplitude	0.0625	0.5625	0.6250	0.5625	1.000	0.9375	1.0000	0.6875	0.4375	0.8750	2
Phase	−157.50	−78.75	112.50	−78.75	−135.00	146.25	146.25	−45.00	−45.00	33.750	
Amplitude	0.4375	0.8125	0.9375	0.8125	0.7500	0.8125	0.5625	0.1250	0.3750	0.5000	3
Phase	157.50	−22.50	56.25	−168.75	56.25	−45.00	112.50	−22.50	−112.50	67.500	
Amplitude	0.3750	0.0625	0.3750	0.6875	0.3125	0.1875	0.2500	0.5000	0.4375	0.8125	4
Phase	−168.75	−22.50	−146.25	146.25	−123.75	−56.25	−56.25	−90.00	11.25	45.00	
Amplitude	0.0625	0.3125	0	0.6250	0.5000	0	0.2500	0.3750	0.0625	0.0625	5
Phase	−135.00	−146.25	−11.25	11.25	−56.25	−78.75	−123.75	33.75	101.25	−56.25	
Amplitude	0.2500	0.5625	0.7500	0.0625	0.3125	0.6875	0.3125	0.4375	0.3125	0.3750	6
Phase	101.25	135.00	−157.50	180.00	−123.75	22.50	90.00	135.00	−67.50	−112.50	
Amplitude	0.8750	0.6250	0.7500	0.1875	0.6250	0.8125	0.6250	0.3750	0.0625	0.5000	7
Phase	101.25	157.50	0	−157.50	157.50	11.25	−146.25	−67.50	−67.50	135.00	
Amplitude	0.9375	0.3125	0.3125	0.5000	0.7500	0.8750	0.8750	0.8125	0.4375	0.0625	8
Phase	112.50	33.75	123.75	157.50	−56.25	−101.25	168.75	135.00	0	−67.50	
Amplitude	0.0625	0.3125	0.1875	0.4375	0.0625	0.3750	0.1250	0.8750	0.9375	0.5625	9
Phase	0	−56.25	135.00	135.00	−135.00	−78.75	−146.25	−78.75	67.50	123.75	

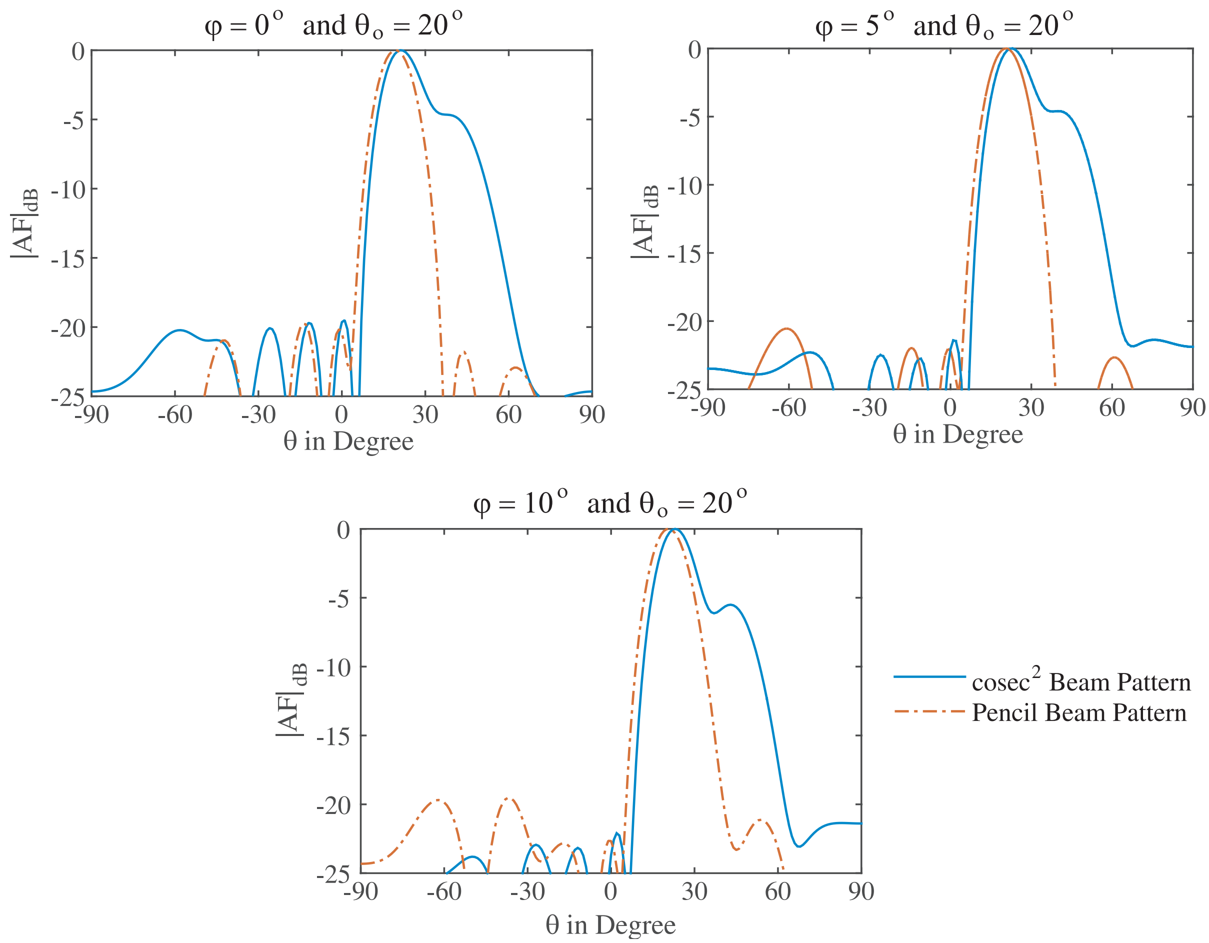

Figure 5. Obtained dual beam patterns at 20° elevation angle using GA for $\varphi = 0°$, $\varphi = 5°$, and $\varphi = 10°$ plane.

In Figures 11, 12, 13, and 14, the beam patterns are generated in three arbitrarily chosen azimuth planes for the same excitations with some minor variation. In each figure, the first arbitrary azimuth angle is chosen as 2.7 degrees ($0° < 2.7° < 5°$ in between the predefined φ plane); the second is 7.8 degrees (within the predefined φ plane 5° and 10°); and the third is 12.1 degrees ($> 10°$ beyond the predefined azimuth plane). Figure 4 shows the array pattern in predefined azimuth planes whereas Figure 11 shows the pattern in arbitrarily chosen azimuth plane, and in both the cases, the optimum excitations are generated using DE. The obtained $cosec^2$ beam patterns follow the desired beam pattern shown in Figure 2 within the coverage range of elevation angle (20° to 50°).

Similarly, (*Figure 5*, *Figure 12*), (*Figure 6*, *Figure 13*) and (*Figure 7*, *Figure 14*) have nearly equal values of the design parameters obtained by using the optimum excitations produced by GA, PSO, and FA for predefined azimuth angle and arbitrary plane.

In Table 2, the values of design parameters are mentioned for the arbitrary angles for all four EAs. The obtained values of design parameters for arbitrarily selected φ planes and predefined φ planes are comparable. So for this array synthesis method, it is not essential to consider all the azimuth planes rather some predefined azimuth planes which ensure a range where the pattern retains the desired characteristic. Figure 15 shows the convergence curves of DE, GA, PSO, and FA. From these convergence curves it is clearly observed that DE is superior to GA, PSO, and FA as fitness value of DE is less than the others. The Computations have been done in MATLAB 2015a with core 2 duo processor, 3 GHz, 4 GB RAM.

Table 6 below compares DE, GA, PSO, and FA performances to design issues. The lowest average

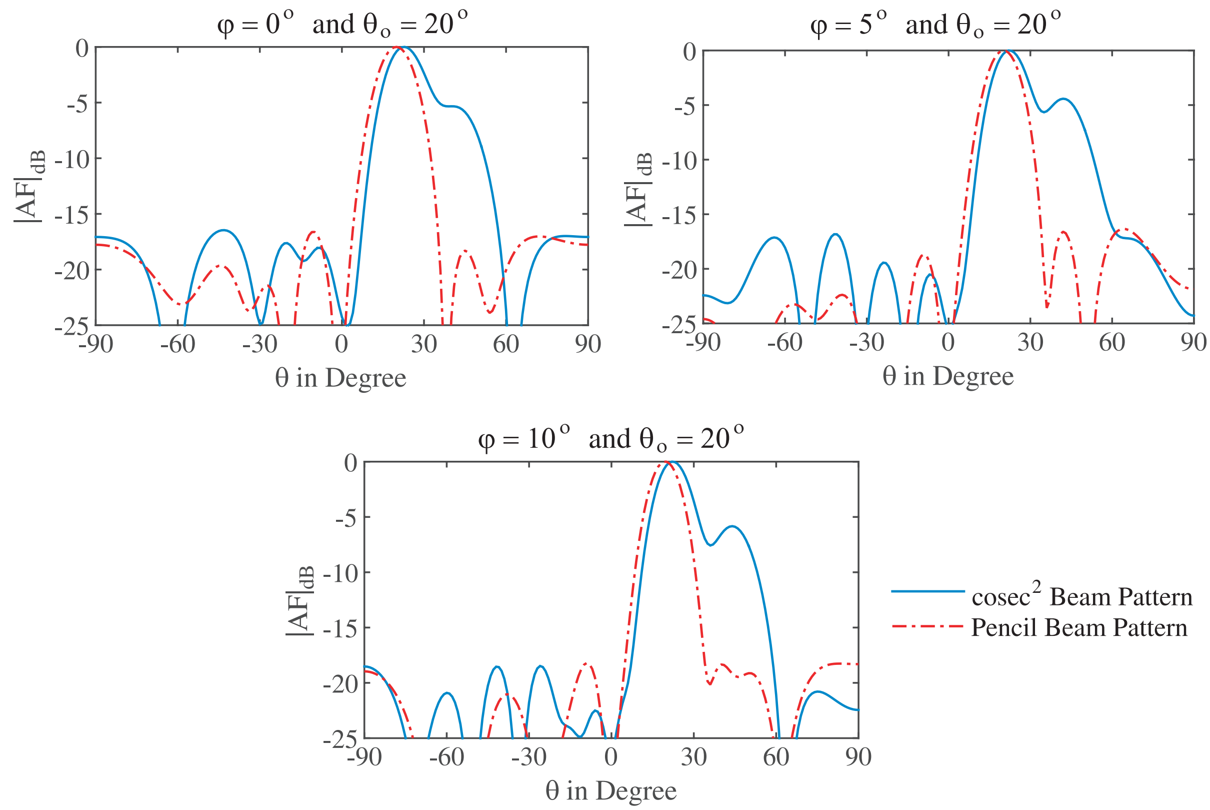

Figure 6. Obtained dual beam patterns at 20° elevation angle using PSO for $\varphi = 0°$, $\varphi = 5°$, and $\varphi = 10°$ plane.

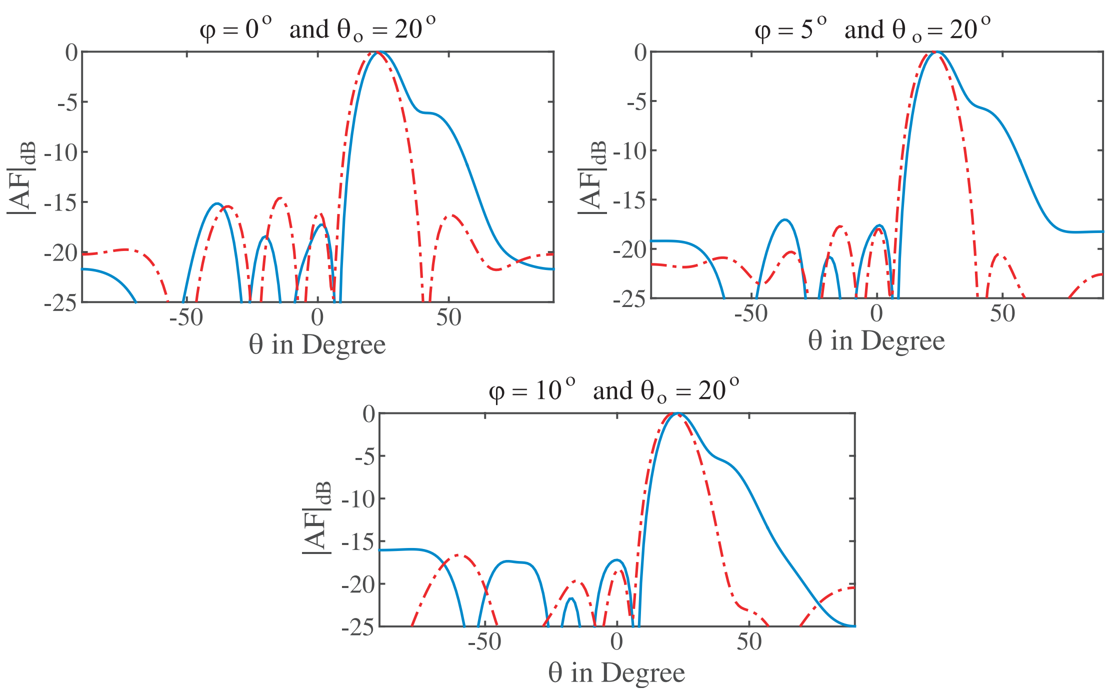

Figure 7. Obtained dual beam patterns at 20° elevation angle using FA for $\varphi = 0°$, $\varphi = 5°$, and $\varphi = 10°$ plane.

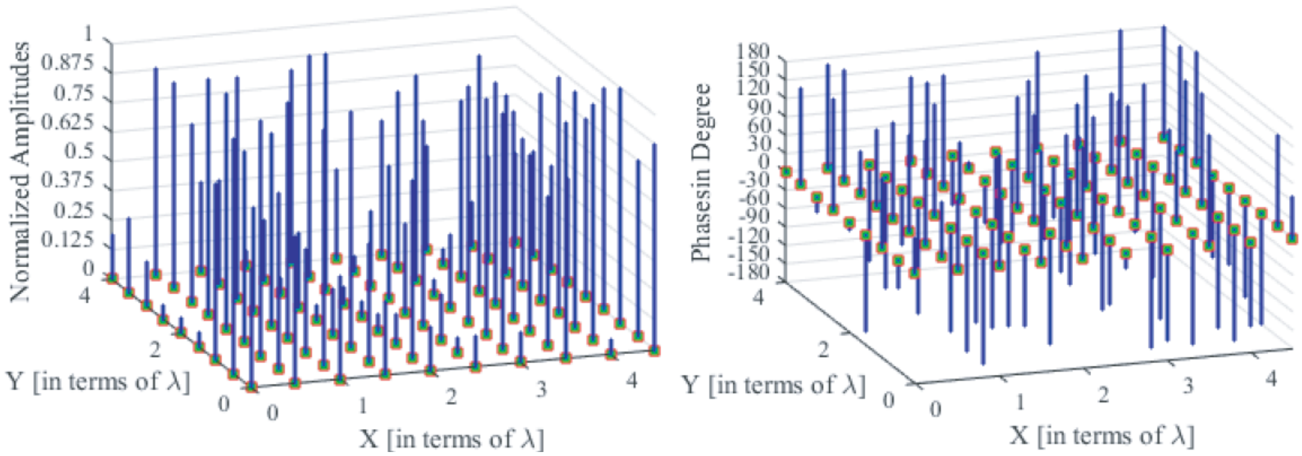

Figure 8. Excitations using DE.

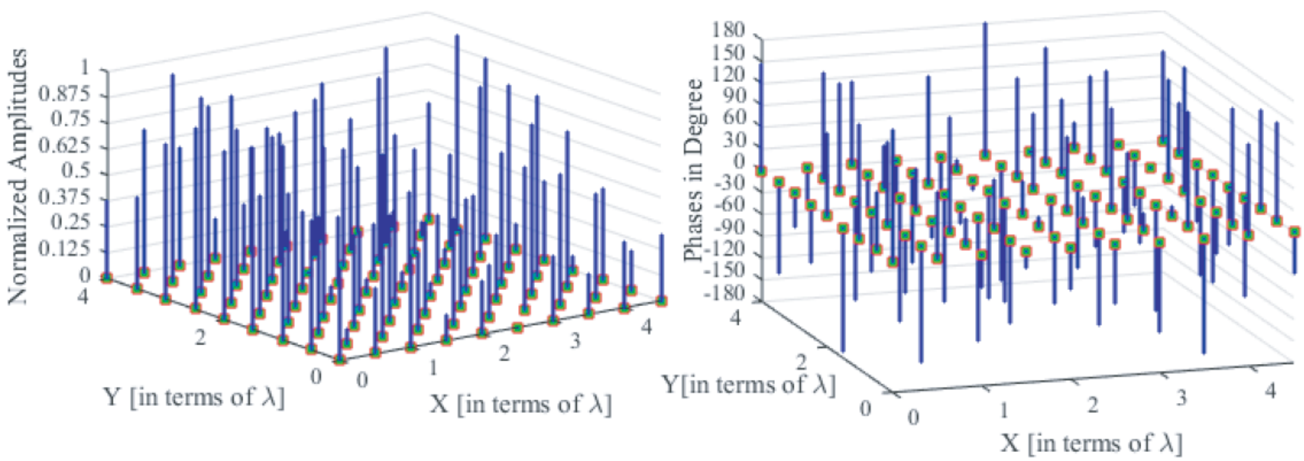

Figure 9. Excitations using GA.

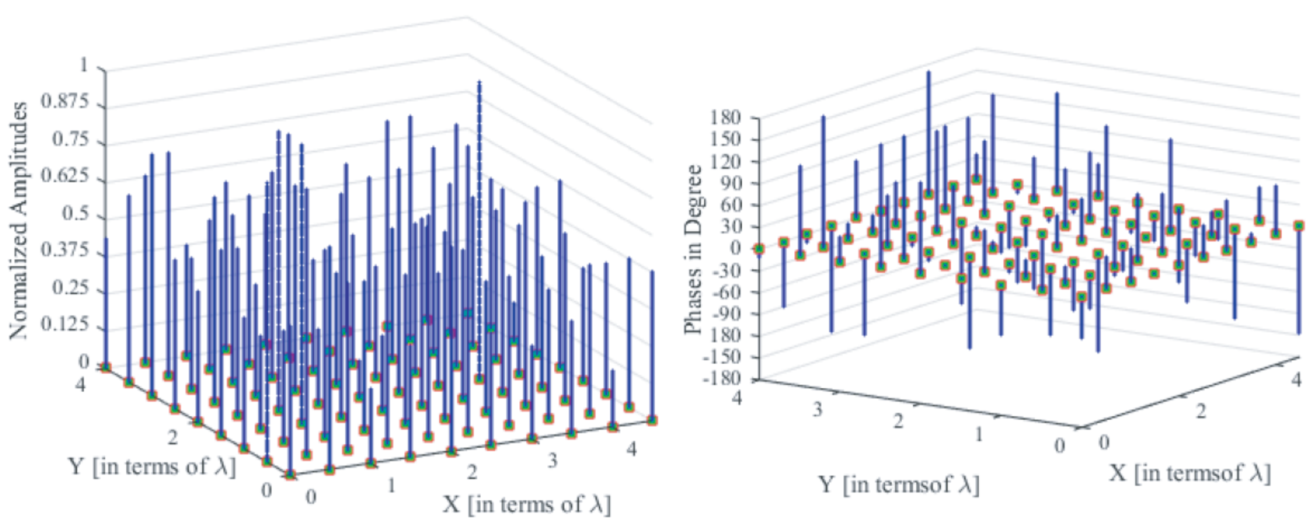

Figure 10. Excitations using PSO.

Table 5. Element wise excitations using Particle Swarm Optimization Algorithm (PSO).

Excitations X → 1	2	3	4	5	5	7	8	9	10	Y↓
Amplitude 0.5000	0.9375	0.4375	0.6250	0.4375	0.5000	0.8125	0.6250	0.4375	0.7500	1
Phase −56.25	67.50	−67.50	−33.75	123.75	101.25	33.75	123.75	−11.25	45.00	
Amplitude 0.5625	0.3750	0.3125	0.5625	0.6875	0.4375	0.7500	0.6250	0.2500	0.5625	2
Phase 22.50	22.50	56.25	0	168.75	−112.50	180.00	−90.00	45.00	−45.00	
Amplitude 0.6250	0.9375	0.9375	0.3750	0.5625	0.5000	0.3750	0.3750	0.5000	0.5000	3
Phase −90.00	−11.25	−123.75	−11.25	67.50	22.50	−11.25	0	45.00	−67.50	
Amplitude 0.7500	0.2500	0.6875	0.6875	0.5625	0.5625	0.6875	0.7500	0.5000	0.2500	4
Phase −45.00	11.25	78.75	−11.25	22.50	−146.25	78.75	90.00	−135.00	45.00	
Amplitude 0.1250	0.3750	0.3750	0.7500	0.4375	0.3750	0.5000	0.6250	0.6250	0.7500	5
Phase −56.25	11.250	135.00	56.250	78.750	45.000	78.750	−33.75	56.250	−78.75	
Amplitude 0.3750	0.4375	0.3125	0.5000	0.3125	0.5000	0.4375	0.5000	0.3750	0.5000	6
Phase −33.75	−90.00	11.250	90.000	67.500	−78.75	0	146.25	78.750	−33.750	
Amplitude 0.4375	0.5625	0.5625	0.3750	0.4375	0.6875	0.6875	1.0000	0.8125	0.6875	7
Phase 101.25	112.50	67.500	11.250	33.750	123.75	−11.25	90.000	−11.250	−56.250	
Amplitude 0.7500	0.6875	0.1875	0.5000	0.5625	0.4375	0.5000	0.5000	0.5000	0.5000	8
Phase 112.50	168.75	67.500	−123.75	−45.00	−33.750	−90.00	−11.25	56.250	135.00	
Amplitude 0.3125	0.5000	0.5000	0.4375	0.3750	0.6250	0.5625	0.1250	0.5000	0.5625	9
Phase −56.25	−146.25	45.000	−33.75	−101.25	−67.50	45.000	135.00	−11.25	33.750	

Table 6. Comparative performance of DE, GA, PSO, and FA.

Algorithm	**Best Fitness (out of 20)**	**Worse**	**Mean**	**Standard Deviation**
DE	56.8813	69.9611	58.9263	3.1810
GA	62.4274	80.5135	66.6496	4.2382
PSO	136.4251	156.456	142.3127	4.9859
FA	190.5110	215.2467	196.5113	5.2668

fitness value of DE relative to GA, PSO, and FA indicates that DE is the best performing algorithm for the problem presented. Table 7 shows the values obtained by the Wilcoxon rank sum test between the DE/GA, DE/PSO, and DE/FA pairs for these design considerations. Any obtained values which are less than 0.05 (5% significance level) are the strongest evidence for the null hypothesis that the best final fitness value obtained by the best algorithm is statistically significant.

Table 7. P-value for Wilcoxon's two sided rank sum test.

Comparison Pair	**P-value**
DE/GA	4.8063e-05
DE/PSO	3.3918e-06
DE/FA	6.2498e-07

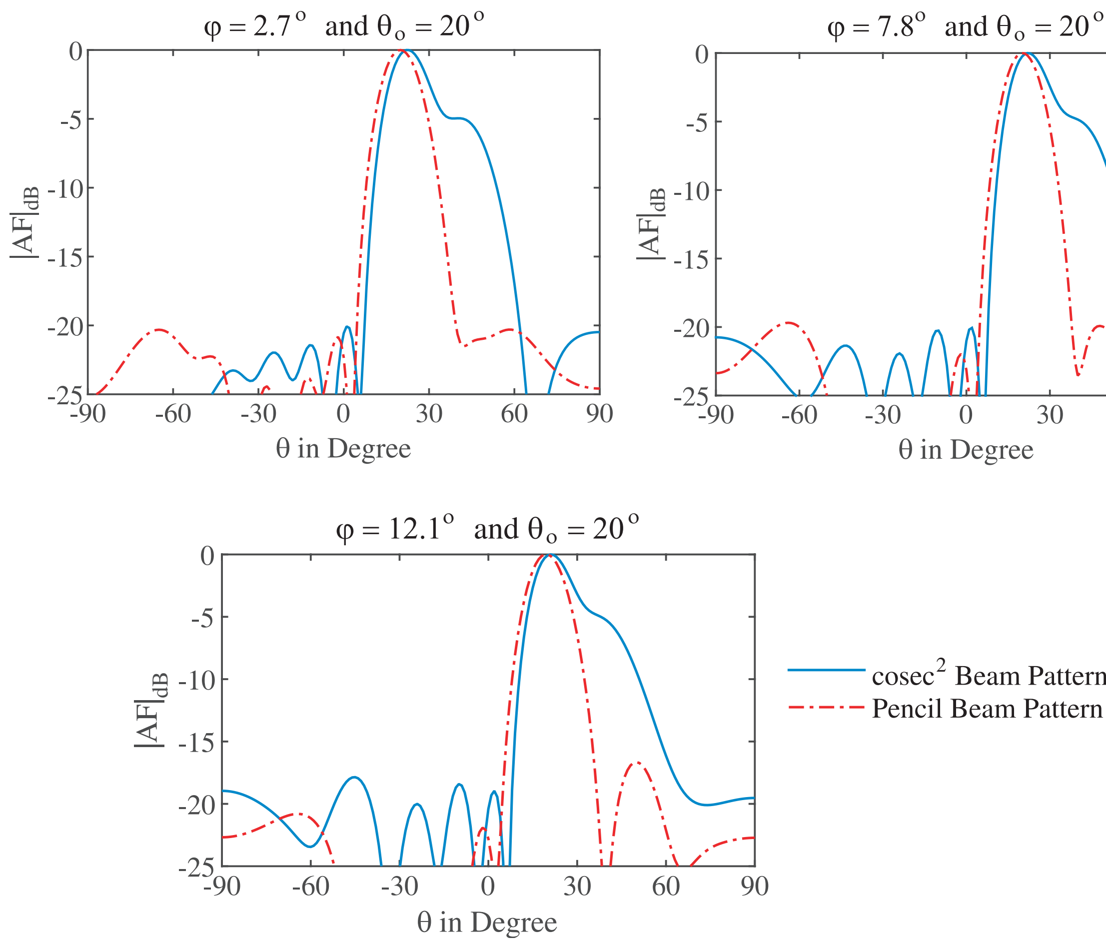

Figure 11. Dual beam patterns at $\theta_o = 20°$ for three arbitrarily chosen φ planes using the same excitations obtained from DE.

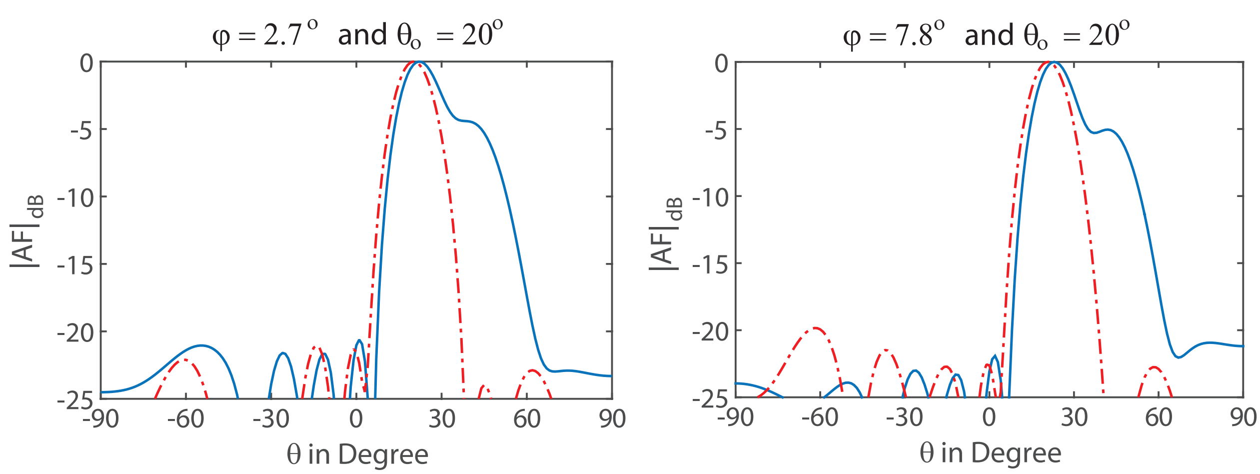

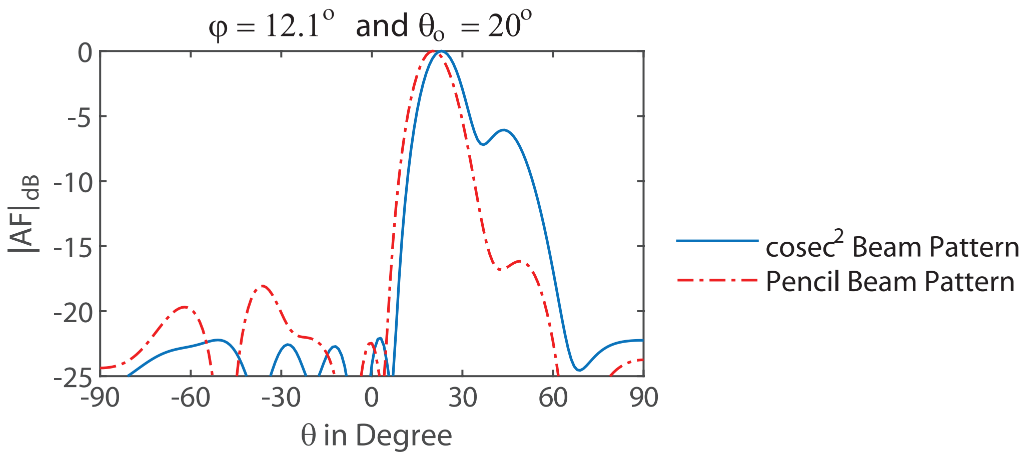

Figure 12. Dual beam patterns at $\theta_o = 20^{\circ}$ for three arbitrarily chosen φ planes using the same excitations obtained from GA.

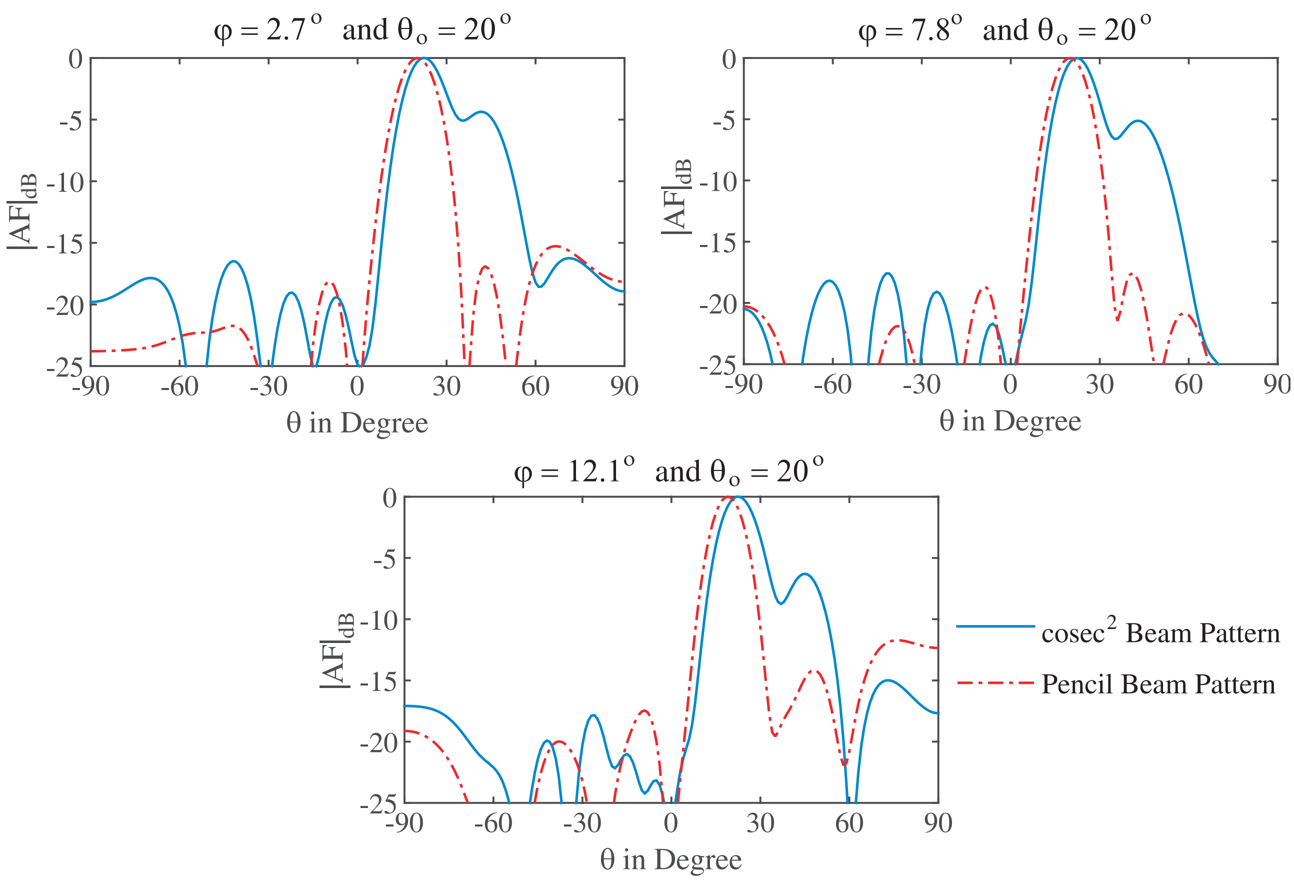

Figure 13. Dual beam patterns at $\theta_o = 20^{\circ}$ for three arbitrarily chosen φ planes using the same excitations obtained from PSO.

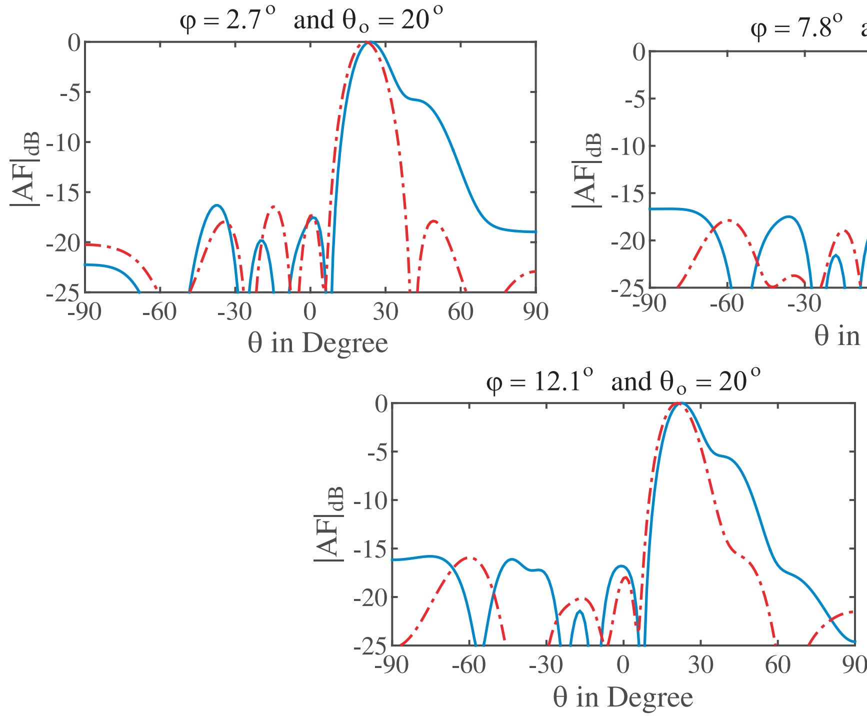

Figure 14. Dual beam patterns at $\theta_o = 20°$ for three arbitrarily chosen φ planes using the same excitations obtained from FA.

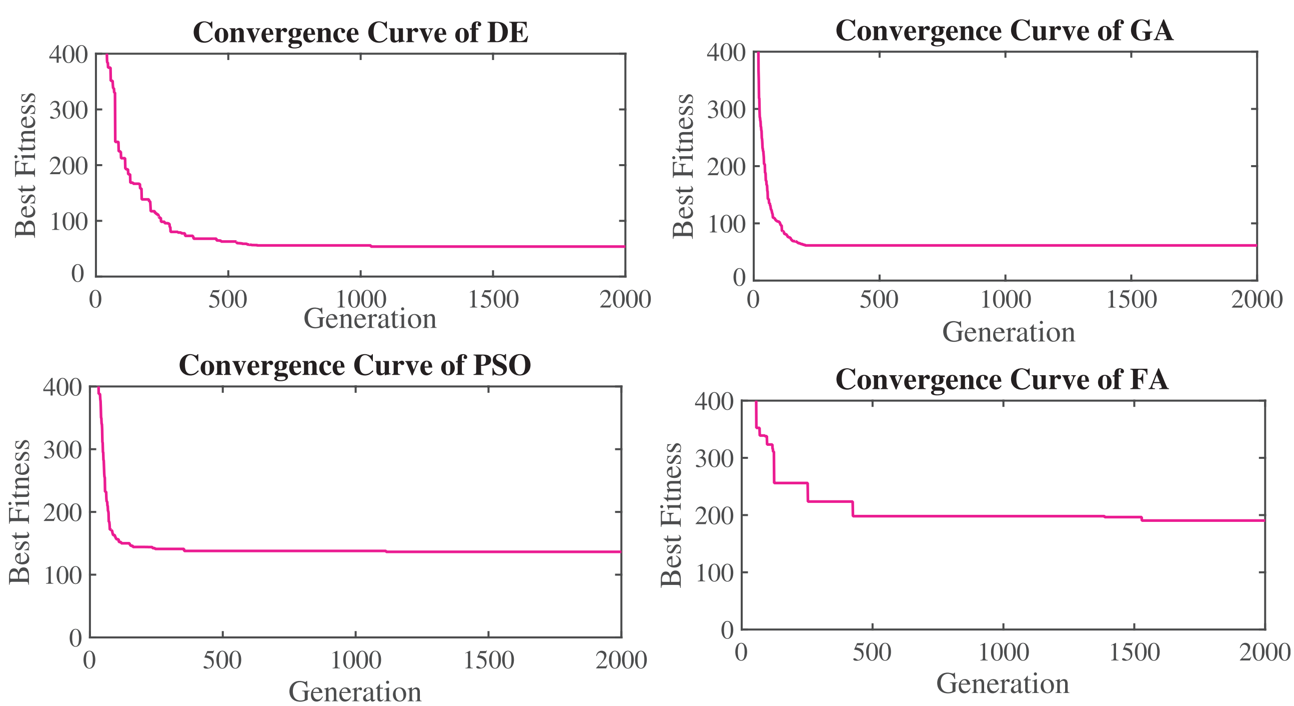

Figure 15. Convergence curve of Differential Evolution Algorithm (DE), Genetic Algorithm(GA), Particle Swarm Optimization Algorithm (PSO) and Firefly Algorithm (FA).

5. CONCLUSION

A steered dual-beam planar array antenna has been synthesized in three different azimuth angles. Two different beam patterns ($cosec^2$ and a pencil beam) are scanned to a particular elevation angle and again synthesized in three predefined azimuth planes using three well known Evolutionary Algorithms. Each Evolutionary Algorithm generates optimum 4-bit discrete amplitudes and 5-bit discrete phases to achieve the desired parameters of the patterns. After selecting and achieving the similar pattern in arbitrary planes, the presented method shows its capability to produce the same beam pattern not only in the predefined azimuth planes rather a range of azimuth planes. The design parameters like peak side lobe level (peak SLL) and ripple Δ are reduced by finding the optimum set of array excitations using DE, GA, and PSO Algorithm. The Dynamic Range Ratio (DRR) is also reduced by using these digital excitations, which results in the smaller number of attenuators and phase shifters in the feed network. This pattern synthesis method also ensures that the desired patterns retain their desired specifications with some minor variations in a range of azimuth plane on the scanning angle also rather in a particular predefined φ plane with zero elevation angle. An acceptable concurrence between the desired and obtained outcomes validated the proposal, and the introduced method can also be used to synthesize other array geometries.

REFERENCES

1. Balanis, C. A., *Antenna Theory, Analysis and Design*, 2nd Edition, Jhon Willy & sons, New York, 1997.
2. Elliott, R. S., *Antenna Theory & Design*, Revised Edition, Wiley-IEEE Press, Dec. 2002.
3. Hansen, R. C., *Phased Array Antennas*, 2nd Edition, Jhon Wiley & Sons, Canada, 2009.
4. Mailloux, R. J., *Phased Array Antenna Handbook*, 2nd Edition, Artech House Antennas and Propagation Library, Boston, 2009.
5. Diaz, X., J. A. Rodriguez, F. Ares, and E. Moreno, "Design of phase-differentiated multiple pattern antenna arrays," *Microwave and Optical Technology Letters*, Vol. 26, No. 1, 52–53, 2000.
6. Lei, J., G. Fu, L. Yang, and D. M. Fu, "Wide band linear printed antenna array with low sidelobe cosecant square-shaped beam pattern," *Progress In Electromagnetics Research C*, Vol. 15, 233–241, 2010.
7. Durr, M., A. Trastoy, and F. Ares, "Multiple-pattern linear antenna arrays with single prefixed amplitude distributions: Modified Woodward-Lawson synthesis," *Electronics Letters*, Vol. 36, No. 16, 1345–1346, 2000.
8. Chatterjee, A., G. K. Mahanti, and R. P. S. Mahapatra, "Design of fully digital controlled reconfigurable dual-beam concentric ring array antenna using gravitational search algorithm," *Progress In Electromagnetics Research B*, Vol. 18, 59–72, 2011.
9. Chatterjee, A., G. K. Mahanti, and A. Chatterjee, "Design of a fully digital controlled reconfigurable switched beam concentric ring array antenna using firefly and particle swarm optimization algorithm," *Progress In Electromagnetics Research B*, Vol. 36, 113–131, 2012.
10. Mandal, D., J. Tewary, K. S. Kola, and V. P. Roy, "Synthesis of dual beam pattern of planar array antenna in a range of azimuth plane using Evolutionary Algorithm," *Progress In Electromagnetics Research Letters*, Vol. 62, 65–70, 2016.
11. Mandal, D., V. P. Roy, A. Chatterjee, and A. K. Bhattacharjee, "Synthesis of dual radiation pattern of rectangular planar array antenna using Evolutionary Algorithm," *ICTACT Journal on Communication Technology*, Vol. 06, No. 03, 1146–1149, 2015.
12. Kenane, E., F. Benmeddour, and F. Djahli, "Nonuniform circular array synthesis for low side lobe level using dynamic invasive weeds optimization," *Progress In Electromagnetics Research C*, Vol. 111, 147–162, 2021.
13. Storn, R. and K. Price, "Differential evolution: A simple and efficient heuristic for global optimization over continuous spaces," *Journal of Global Optimization*, Vol. 11, No. 04, 341–359, 1997.

14. Price, K. V., R. M. Storn, and J. A. Lampinen, *Differential Evolution — A Practical Approach to Global Optimization. Natural Computing*, Springer, New York, USA, 2005.
15. Das, S., A. Abraham, U. K. Chakraborty, and A. Konar, "Differential evolution using a neighborhood-based mutation operator," *IEEE Transactions on Evolutionary Computation*, Vol. 13, No. 03, 526–553, 2009.
16. Guo, J. and J. Li, "Pattern synthesis of conformal array antenna in the presence of platformusing differential evolution algorithm," *IEEE Transactions on Antennas and Propagation*, Vol. 57, No. 09, 2615–2621, 2009.
17. Qi, X., Z. Huang, and Y. Chen, "An improved differential evolution algorithm based on adaptive parameter," *Journal of Control Science and Engineering*, Vol. 2013, 2013.
18. Yang, S., Y. B. Gan, and A. Qing, "Sideband suppression in time-modulated linear arrays by the differential evolution algorithm," *IEEE Transactions on Antennas and Propagations Letters*, Vol. 1, No. 1, 173–175, 2002.
19. Massa, A., M. Pastorino, and A. Randazzo, "Optimization of the directivity of a monopulse antenna with a subarray weighting by a hybrid differential evolution method," *IEEE Transactions on Antennas and Propagations Letters*, Vol. 5, No. 1, 155–158, 2006.
20. Kennedy, J. and R. C. Eberhart, "Particle swarm optimization," *Proceedings of the Conference on Neural Networks*, 1942–1948, Perth, Australia, 1995.
21. Shi, X. H. and R. C. Eberhart, "Empirical study of particle swarm optimization," *Proceedings of the Congress on Evolutionary Computation*, 1945–1950, Washington, D.C., USA, 1999.
22. Juang, C. F., "A hybrid of genetic algorithm and particle swarm optimization for recurrent network design," *IEEE Trans. Syst., Man, Cybern. — Part B: Cybern.*, Vol. 34, 997–1006, 2004.
23. Robinson, J. and Y. Rahmat-Samii, "Particle swarm optimization in electromagnetics," *IEEE Transactions on Antennas and Propagation*, Vol. 52, No. 2, 397–407, 2004.
24. Boeringer, D. W. and D. H. Werner, "Particle swarm optimization versus genetic algorithms for phased array synthesis," *IEEE Trans. Antennas Propagat.*, Vol. 52, 771–779, 2004.
25. Lee, K. C. and J. Y. Jhang, "Application of particle swarm algorithm to the optimization of unequally spaced antenna arrays," *Journal of Electromagnetic Waves and Applications*, Vol. 20, No. 14, 2001–2012, 2006.
26. Carro Ceballos, P. L., J. De Mingo Sanz, and P. G. Ducar, "Radiation pattern synthesis for maximum mean effective gain with spherical wave expansions and particle swarm techniques," *Progress In Electromagnetics Research*, Vol. 103, 355–370, 2010.
27. Modiri, A. and K. Kiasaleh, "Modification of real-number and binary PSO algorithms for accelerated convergence," *IEEE Transactions on Antennas and Propagation*, Vol. 59, 214–224, 2011.
28. Haupt, R. L., "Introduction to genetic algorithms for electromagnetics," *IEEE Antennas and Propagation Magazine*, Vol. 37, No. 2, 7–15, 1995.
29. Man, K. F., K. S. Tang, and S. Kwong, "Genetic algorithms: Concepts and applications," *IEEE Transactions on Industrial Electronics*, Vol. 43, No. 5, 519–534, 1996.
30. Johnson, J. M. and Y. Rahmat-Samii, "Genetic algorithms in engineering electromagnetics," *IEEE Antennas and Propagation Magazine*, Vol. 39, No. 4, 7–21, 1997.
31. Marcano, D. and F. Duran, "Synthesis of antenna arrays using genetic algorithms," *IEEE Antennas and Propagation Magazine*, Vol. 42, No. 3, 12–20, 2000.
32. Panduro, M. A., A. L. Mendez, R. Dominguez, and G. Romero, "Design of non-uniform circular antenna arrays for side lobe reduction using the method of genetic algorithms," *International Journal of Electronics and Communications*, Vol. 60, No. 10, 713–717, 2006.